

## Density of States of Ni: Soft-X-Ray Spectrum and Comparison with Photoemission and Ion Neutralization Studies

J. R. CUTHILL, A. J. MCALISTER,\* AND M. L. WILLIAMS

*Institute for Materials Research, Metallurgy Division, National Bureau of Standards, Washington, D. C.*

AND

R. E. WATSON†

*Brookhaven National Laboratory,‡ Upton, New York*

(Received 24 July 1967)

Soft-x-ray studies have been made on paramagnetic Ni and interpreted in terms of the single-particle density of states. In particular, the  $M_{2,3}$  emission spectrum has been investigated, using improved experimental techniques. Measurements were made at 960°C, at an average pressure of  $5 \times 10^{-8}$  Torr, using an oxide-free surface. Fine structure was observed in the spectrum. Although first-principles correction of self-absorption effects and satellite and subband overlap is not yet possible, careful consideration is given them, with the result that the  $M_3$  band can be resolved from the accompanying structure in a plausible way. Most of its features can be taken with reasonable confidence to be characteristic of the true  $M_3$  emission band. Comparison is made with earlier soft-x-ray results, with band calculations for paramagnetic Ni, and with ion neutralization and photoemission measurements on ferromagnetic Ni. Systematic variations in transition matrix elements and lifetime broadening appear important when relating any experiment with theory, and an aspect of each of these problems has been considered quantitatively. The variation obtained is more severe for the photoemission than for the soft-x-ray analysis. The ion-neutralization and soft-x-ray results appear closer to the single-particle density of states.

### I. INTRODUCTION

DETAILED and increasingly realistic calculations of the electronic energy levels of the transition metals are being carried out.<sup>1-7</sup> Predictions of the Fermi surfaces of a variety of transition metals are in gratifying agreement with experiment. However, a full test of single-particle band theory requires inspection of structure off the Fermi energy, and experimental probes of the deeper-lying states are most desirable. Optical-constants measurements provide one source of such information. Photoemission (PES)<sup>8</sup> and ion-neutralization spectroscopy (INS)<sup>9</sup> are proving valuable as probes of the density of states in these materials. The traditional tool in density-of-states investigations, soft-x-ray spectroscopy (SXS), has been advanced by the application of modern high vacuum and photon counting techniques. We have applied these techniques to the measurement of the  $M_{2,3}$  emission spectrum of para-

magnetic, oxide-free Ni, and have been able to resolve previously unreported fine structure.<sup>10</sup> The results are relevant to the single-particle description of metallic Ni.

The  $M_3$  band is resolved out of the  $M_{2,3}$  spectrum in a plausible way and is compared with earlier SXS studies of Ni, with various band-theory predictions of the density of states of paramagnetic Ni, and finally with the results of INS and PES studies on ferromagnetic Ni. (Since INS and PES measurements show no significant changes when Ni is raised above its Curie temperature,<sup>8,9</sup> the difference in magnetic state should not seriously affect this comparison.) Crude agreement in such gross features as  $d$ -band width is seen between the various experiments and theory. Systematic variation in transition probabilities (which are usually assumed constant) are found to warp the experimental curves (as do dynamical or multiparticle effects) and detailed agreement cannot be expected—and is not seen—between theoretical densities of states and *any* experimental curve with these factors present. Two aspects of this problem will be considered quantitatively. As significant as any discrepancy between theory and experiment are the discrepancies between experiments. It appears that multiparticle effects and strongly varying transition probabilities are more important to and have yet to be resolved out of the PES curves, causing them to be a poorer representation of the single-particle density of states than are those obtained in INS and SXS. Given the INS and SXS results, the single-particle picture is in some ways a quite (perhaps surprisingly) adequate description of the elec-

\* National Academy of Sciences-National Research Council postdoctoral research associate, 1967.

† Also, consultant, National Bureau of Standards.

‡ Supported by U. S. Atomic Energy Commission.

<sup>1</sup> J. H. Wood, *Phys. Rev.* **126**, 517 (1962).

<sup>2</sup> L. F. Mattheis, Massachusetts Institute of Technology, quarterly Progress Report no. 48, p. 5, 1963 (unpublished).

<sup>3</sup> J. G. Hanus, Massachusetts Institute of Technology, quarterly Progress Report no. 44, p. 29, 1962 (unpublished).

<sup>4</sup> L. Hodges, H. F. Ehrenreich, and N. D. Lang, *Phys. Rev.* **153**, 574, (1966).

<sup>5</sup> S. Wakoh and J. Yamashita, *J. Phys. Soc. Japan* **19**, 1342, (1964).

<sup>6</sup> E. C. Snow, T. J. Waber, and A. C. Switendek, *J. Appl. Phys.* **37**, 1342 (1966).

<sup>7</sup> J. W. D. Connolly, Massachusetts Institute of Technology, quarterly Progress Report no. 62, p. 3, 1966 (unpublished).

<sup>8</sup> A. J. Blodgett and W. E. Spicer, *Phys. Rev. Letters* **15**, 29 (1965); *Phys. Rev.* **146**, 390 (1966).

<sup>9</sup> H. D. Hagstrum and G. E. Becker, *Phys. Rev. Letters* **16**, 230, (1966); *Phys. Rev.* **59**, 572 (1967).

<sup>10</sup> A preliminary report on these results was given by J. R. Cuthill, A. J. McAlister, and M. L. Williams, *Phys. Rev. Letters* **16**, 993 (1966).

tronic structure off the Fermi surface of metallic Ni. Further comparison of any of the experiments with single-particle theory requires theoretical estimates of such factors as transition probabilities, and in particular, their variation through the conduction bands.

## II. EXPERIMENTAL

The sample studied was a polycrystalline Ni rod of stated purity 99.995%. Spectrographic analysis showed metallic contaminant content to be less than 10 ppm. Pressure in the sample region during measurements ranged from  $2 \times 10^{-8}$  to  $8 \times 10^{-8}$  Torr. Excitation was by electron bombardment at constant 2.5-keV beam energy. A fair degree of thermal isolation was achieved by mounting the samples on insulators and using a thin electrical lead. Temperature was held at  $(960 \pm 7)^\circ\text{C}$  by small variations of the electron beam current. Temperature was measured with a Pt-Pt 10% Rh thermocouple spot welded to the sample, and positioned just outside of the area observed by the spectrometer. Rotation of the sample at full operating conditions produced no change in recorded temperature, and this procedure is therefore believed to give an accurate indication of the temperature in the region of excitation.

The spectrometer is a Rowland mount, with a 2-m, lightly ruled Siegbahn concave grating at  $2^\circ$  incidence. A strip photomultiplier detector is employed with entrance and exit slits 0.1-mm wide. A mechanical drive system moves the detector along the Rowland circle, with the plane of the detector slit always normal to the chord joining the slit and the grating. Thus, a constant geometric resolution of 0.5 Å is achieved with the slit widths used. The lead screw was calibrated with the Al  $L_3$  absorption edge energy of Tomboulian,<sup>11</sup> with the specific aim of making our energy scale correspond with his, so that we might use his Ni absorption data in the interpretation of our results. While rough, this calibration is adequate for our present purposes. The spectrum was swept continuously, and data were taken and recorded both digitally and on a ratemeter driven strip chart recorder. Successive runs, made under as nearly identical conditions as possible, were summed to enhance signal-to-noise ratio. A separate paper describing the apparatus is being submitted for publication, and no further instrumental details will be given here.

The question of surface cleanliness can be dealt with straightforwardly. Only two contaminants need be considered: carbon from cracked residual vacuum pump oil and the electron gun filament, and oxygen. Nickel carbides are quite weakly bound, and in our experimental temperature range, carbon will be present only as an inert surface deposit. It will therefore reduce the intensity of the Ni spectrum by competing for the available exciting electrons, and will emit its own emission spectrum in first and higher orders. The third-order

carbon peak appeared at moderate intensity, well away from the Ni band. The fourth-order peak, which should occur at 69.7 eV, just above the Ni peak was not observed. Calculations of grating efficiency in fourth order, based on the work of Sprague *et al.*,<sup>12</sup> indicate that it should not appear. The nature of oxygen-nickel complexes on various Ni crystal faces has been thoroughly studied by low-energy electron diffraction.<sup>13</sup> This work indicates that at our experimental pressure, and below  $830^\circ\text{C}$ , crystallites of bulk NiO are present on the surface. Above this temperature, NiO dissociates, and monolayer arrays of oxygen are bound in the several single crystal Ni surfaces. Above  $830^\circ\text{C}$ , these monolayers dissociate on all except the (110) Ni surface, and even here prolonged heating may partially remove the last oxygen layer. We have accordingly studied the Ni  $M_{2,3}$  emission spectrum at 740, 870, and  $960^\circ\text{C}$ , always at 2.5-keV electron beam energy, and at a beam current appropriate to the desired temperature. Three quite distinct spectra were observed. While only the  $960^\circ\text{C}$  spectrum was intensively studied, it was established that at  $870^\circ\text{C}$ , where a fairly complete monolayer coverage should exist, the high-energy side of the emission band was somewhat broadened while on the low-energy side considerable loss of detail occurs. At  $740^\circ\text{C}$ , where monolayers of oxide are complete and extensive deposits of bulk NiO crystallites should be present, all fine structure is washed out and the band is much wider. These changes are almost surely associated with the nature of the surface oxide layer, and with the probable shallow electron beam penetration of the sample in our experimental arrangement. This last point will be discussed below in the treatment of sample self-absorption. The emission spectrum at  $960^\circ$  is characteristic of a Ni surface, free of oxide save for a partial monolayer of any exposed (110) crystallite face. Since the data at lower temperatures are of interest only in connection with this point they are not presented here. It may be, however, that SXS will be useful tool in the study of surface oxidation.

## III. ANALYSIS

In Fig. 1, the measured  $M_{2,3}$  emission band of Ni at  $960^\circ\text{C}$  and 2.5-keV electron excitation is shown. This spectrum is the sum of 44 separate runs, each taken under nearly identical conditions. The error bars shown represent 50% confidence level,  $\pm 0.7\sqrt{N}$ , where  $N$  is the total number of counts in a given energy interval. Also shown in this figure is the smoothed spectrum, with a background correction fitted above and below the emission band and then subtracted off. This correction is consistent with our observations of the continuum of neighboring elements, and with the  $\lambda^{-2}$  in-

<sup>12</sup> G. Sprague, D. H. Tomboulian, and D. E. Bedo, *J. Opt. Soc. Am.* **45**, 756 (1955).

<sup>13</sup> L. H. Germer, C. D. Hartman, A. U. MacRae, and E. J. Schreiber, Bell Telephone System, Technical Publication Monograph no. 4364, 1963 (unpublished).

<sup>11</sup> W. H. Cady and D. H. Tomboulian, *Phys. Rev.* **59**, 381 (1941).

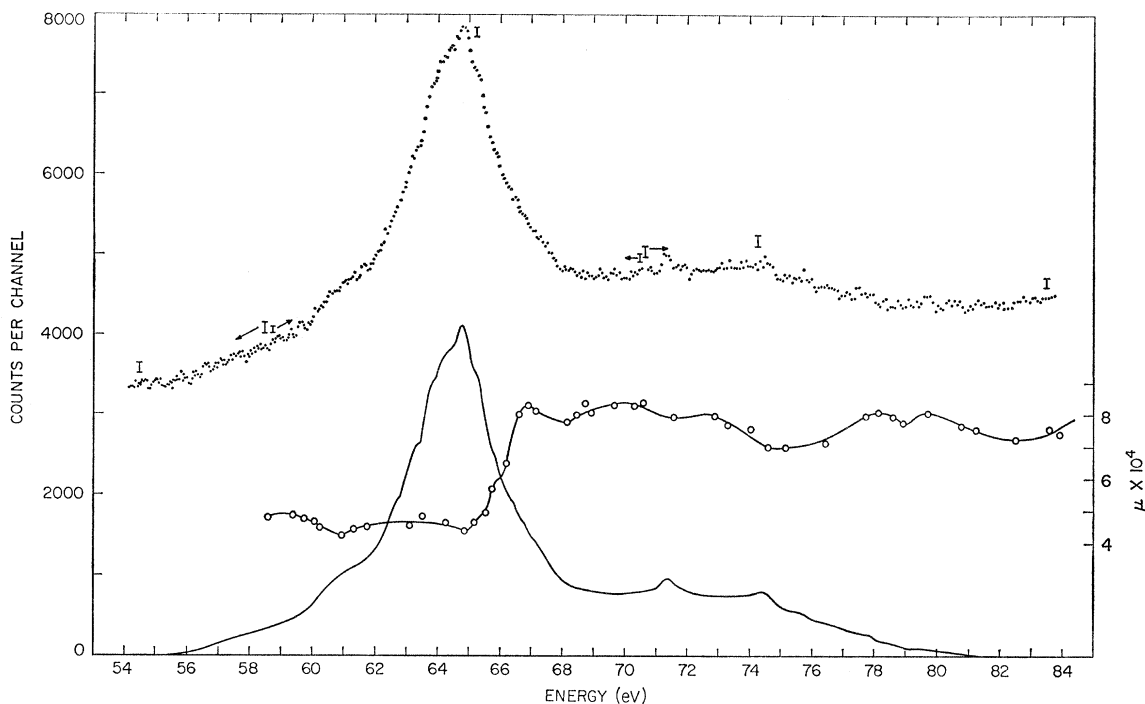


FIG. 1. The upper curve shows the raw data. The error bars represent 50% confidence level. The error is larger in the high- and low-energy tail regions because only 60% of the runs covered the entire energy interval. The data in the tail regions were scaled to fit smoothly on to the more accurately known central region. The lower curve is the smoothed and background-corrected curve used in our analysis. The center curve is the mass absorption coefficient of Ni as measured by Tomboulian *et al.* (Ref. 17).

tensity behavior expected in this spectral region,<sup>14</sup> when the calculated grating reflectivity<sup>12</sup> and diffuse scattering from the grating are considered. It is impossible to calculate the background exactly, but these considerations give us confidence in the general reliability of this correction procedure. The possibility of structure in the background at the  $M_{2,3}$  absorption edge will be dealt with below in our discussion of sample self-absorption.

Further treatment of the data must be done cautiously. The spectrum is a complex of overlapping  $M_2$  and  $M_3$  bands and high-energy satellites. We wish to extract the  $M_3$  spectrum from this tangle and compare it with the calculated density of states of paramagnetic Ni and with the results of other experimental techniques which should reflect the density of states. This problem, difficult enough in itself, is further complicated by the possibility of strong self-absorption in the sample. Still, enough corollary information is available to enable us to carry out the resolution process in a plausible way, and to obtain a reasonable representation of the  $M_3$  emission band. We deal with these problems in their natural order.

First, we must decide to what extent the spectrum is distorted by self-absorption. The maximum practical range (that thickness which a barely detectable number of electrons will penetrate) of 2.5-keV electrons in

Ni is known to be about 350 Å.<sup>15</sup> Owing to severe multiple scattering, only a few electrons penetrate this far; the average electron will reach only about one-half this depth. Furthermore, in our experimental arrangement, the exciting electron beam strikes the sample at an angle of 15–30° from the sample surface. Of course, the question of whether this results in a shallower penetration of the sample must be asked, since multiply scattered electrons can quickly lose all sense of initial direction. The only direct work known to us on this point in an energy range near our own is that of Bonnelle.<sup>16</sup> In this work on the  $L_3$  emission and absorption spectrum of Ni, the electron beam and photon take off directions for emission work were perpendicular, and the flat sample was rotated, so that beam incidence angle decreased as take off angle increased. Then, with absorption coefficients determined in the same work, corrections were made on data taken at high incidence and low take off for self-absorption, and quite good agreement found with data taken at low incidence and high take off. While the effects of incidence angle and take off angle were not checked independently, the agreement would have been noticeably worse if take off alone were considered. The range of electron beam voltages considered included our own value of 2.5 keV. Thus, even though the Ni  $L_3$  threshold is about a factor of ten

<sup>15</sup> C. Feldman, Phys. Rev. **117**, 455 (1960).

<sup>14</sup> S. T. Stephenson and F. D. Mason, Phys. Rev. **75**, 1171 (1949).

<sup>16</sup> C. Bonnelle, Doctoral thesis, University of Paris, 1964 (unpublished).

greater than that of Ni  $M_{2,3}$ , a noticeably shallower target penetration results for low angles of electron beam incidence. In our own laboratory, we have looked for evidence of self-absorption in NiAl<sub>3</sub> by comparing the emission intensities just below the Al and Ni absorption edges at 1.5, 2.0, and 2.5 keV. A rather strong effect is expected if the low electron-beam incidence angle is ineffective in reducing the sample penetration depth. No evidence of self-absorption was observed. An effective emission depth in Ni at 2.5 keV of about 80 Å seems to be indicated by these considerations. Hence, if self-absorption corrections are referred to 60.0 eV, using Tomboulia's Ni absorption data<sup>17</sup> shown in Fig. 1 as a basis for estimates, then above 65.0 eV, self-absorption effects should never exceed 10%, while below this energy they should be completely negligible. As a final point we should note that the high-energy absorption structure shown in Tomboulia's absorption curves for Ni are not reflected in our total emission curve. While his measurements were undoubtedly made on a ferromagnetic sample, the effects of exchange splitting should be small. No indisputable correlation is seen and we take this as evidence against any noticeable self-absorption effects in our measurements. This is true of both characteristic and bremsstrahlung emission, even though the effective depth of emission should be different in each case. As a final remark here, we note that the sensitivity of our data to surface conditions is indicative of fairly shallow penetration. Indeed, our data may be more seriously affected by surface properties of Ni than by self-absorption in the sample.

The low-intensity, high-energy tail structure is in all likelihood composed of multiple ionization satellites. Two definite peaks appear at 71.4 and 74.4 eV. The mean separation of these peaks from the main band suggests that they result from an extra vacancy in the  $3p$  shell. (Compare the 8 eV separation to the difference in  $3p$  binding energy of Ni and Cu of 7 eV.)<sup>18</sup> The removal of a second  $3p$  electron should give rise to a triplet  $P$  state, with degeneracy removed by spin-orbit interaction. Satellites arising from the transition of  $s$ - $d$  valence electrons into these levels should dominate the satellite structure, and we will neglect others. If we assume zero core contraction, the splitting of the triplet  $P$  levels, in the intermediate coupling approximation<sup>19</sup> is estimated to be 1.25,  $-1.05$ , and  $-1.25$  eV, which gives rise to one distinct and two unresolved satellites, with separation of 2.5 eV. This result is in reasonable agreement with the observed splitting, in view of our neglect of core contraction. Each of these satellites may consist of a family of satellites, due to interaction with

the valence electrons. Such splitting should be quite small since the peaks are reasonably distinct. In cases where multiple ionization satellites are clearly resolved, they are somewhat broader than the main band but otherwise faithful reproductions of it.<sup>20</sup> While this interpretation of the satellites is only tentative, it seems quite reasonable to assume the main part of the satellite structure to consist of two bands, facsimiles of the main band, scaled down and shifted to higher energy. Auger filling of the  $M_2$  level from the  $M_3$  is also expected to produce satellite smearing of the Fermi edge. Such structure was clearly observed in the  $L_3$  emission spectrum by Chopra and Liefeld,<sup>21</sup> who studied the spectrum as a function of electron-beam voltage above and below  $L_2$  threshold. This satellite structure in the  $L$  spectrum disappears below  $L_2$  threshold, and when present, appears to have no effect on the shape of the emission band below the Fermi energy. We assume this to be true for the  $M$  spectrum as well, and make no attempt to correct for it.

Our task is to resolve the  $M_3$  band from a complex of four overlapping bands, the  $M_2$ ,  $M_3$ , and two dominant satellites in the high-energy tail, all assumed to have the same shape, but differing in location and scale. To resolve two overlapping bands of identical shape, one shifted up in energy by  $\epsilon$  and scaled by  $\alpha$ , we may use the expression<sup>22</sup>

$$M_3(E) = \sum_{n=0}^N (-\alpha)^n M_{2,3}(E - n\epsilon); \quad N \leq (E - E_0)/\epsilon,$$

where  $N$  is rounded to the nearest positive integer or zero, and  $E_0$  is the energy at the bottom of the complex. A first approximation to the  $M_3$  band shape may be obtained by noting that the first peak in the smoothed complex occurs 9 eV above  $E_0$ , and approximating the bottom of the two satellite complex by extrapolating the intensity from 71.4 to zero at 62.4. This is subtracted off and the resulting approximate  $M_{2,3}$  complex resolved. The resulting first approximation to the  $M_3$  band is then used to fit the satellite structure. This is subtracted to yield a second approximation to the  $M_{2,3}$  complex, which is resolved to give a second approximation to the  $M_3$  band. Several repetitions lead to an unchanging  $M_3$  band shape. This approach is rough. Only the major structures in the satellite tail are considered. Broadening of the satellites by shorter inner level lifetime and possible interaction with valence electrons, and tailing of the Fermi edge by multiple valence band hole satellites (expected to be more pronounced in the  $M_3$  than the  $M_2$ ) are neglected. Only the extreme tail of the major satellite components overlaps the  $M_3$  band, however, and the error expected in the resolved  $M_3$  band

<sup>17</sup> D. H. Tomboulia, D. E. Bedo, and W. M. Neupert, *J. Chem. Phys. Solids* **3**, 282 (1957).

<sup>18</sup> S. Hagstrom, C. Nordling, and K. Siegbahn, in *Alpha, Beta, and Gamma Ray Spectroscopy*, edited by K. Siegbahn (North-Holland Publishing Company, Amsterdam, 1965), Vol. I, p. 845.

<sup>19</sup> E. U. Condon and G. H. Shortley, *The Theory of Atomic Spectra* (Cambridge University Press, Cambridge, England, 1935), Chap. 11.

<sup>20</sup> J. A. Caterall and J. Trotter, *Phil. Mag.* **3**, 1424 (1958).

<sup>21</sup> D. R. Chopra, Doctoral thesis, New Mexico State University, 1964 (unpublished).

<sup>22</sup> This expression is obtained by inverting the expression for the intensity of two overlapping bands,  $M_{2,3}(E) = M_3(E) + \alpha M_3(E - \epsilon)$ .

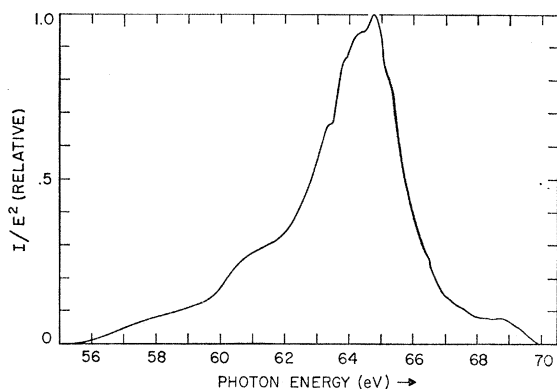


FIG. 2. The resolved  $M_3$  band, normalized to peak value.

from neglecting these features should be only a small uncertainty in the peak amplitude.

The splitting of the  $M_2$  and  $M_3$  bands  $\epsilon$  was estimated in several ways. Extrapolation of the Sommerfeld term energy expression to  $Z=28$ , using the  $M$ -shell screening number for  $Z>33$ , gives a value of 1.96 eV.<sup>23</sup> The  $L_3$  and  $L_2$  absorption edges of Ni show a sharp "white line," presumably due to a large unfilled state density above  $E_F$ .<sup>16</sup> Similar structure is expected in the overlapping  $M_{2,3}$  absorption spectrum,<sup>17</sup> and the first two peaks there are 1.8 eV apart, suggesting a splitting of this value or a somewhat greater splitting. The partially resolved structure on the leading edge of the emission band indicates that  $\epsilon$  lies in the range of 1.8 to 2.0 eV (as well as an  $\alpha$  value of about 0.3). Finally, if the  $K\beta_{13}$  emission line is assumed to consist of two overlapping Lorentzian lines, of the same width, with  $K\beta_3$  one half as intense as  $K\beta_1$ ,  $\epsilon$  is estimated from the observed asymmetry index and width at half maximum<sup>24</sup> to be about 1.8 eV. The ratio of  $M_2$  to  $M_3$  intensity  $\alpha$  is expected to be  $<0.5$ , the population ratio of  $3p^{1/2}$  to  $3p^{3/2}$  states (allowing for the expected reduction below 0.5 by Auger filling of  $M_2$  holes from  $M_3$ ).

The resolution procedure was carried out for an  $\epsilon$  range of 1.8 to 2.0 eV, and  $\alpha$  from 0.5 to 0.1. Choices of  $\alpha>0.35$  result in definite physical inconsistencies, but otherwise, results were quite insensitive to the choice of these parameters. Below 65.0 eV, amplitude in the region of the peak varied by about 10% with very slight changes in the location and definition of the fine structure. Above 65.0 eV, the residual satellite tail appeared, and its shape and magnitude were somewhat sensitive to the satellite correction and unfolding process; but for reasons cited above, this is of no consequence to our investigation. The resolved  $M_3$  band shown in Fig. 2 is characteristic of an  $\epsilon$  range of 1.8 to 2.0 eV, and  $\alpha$  of 0.2 to 0.3.

We now turn our attention to the role played in SXS by many-body and/or collective processes, whose possi-

ble importance was cautiously discussed by Parratt,<sup>25</sup> and which Spicer<sup>26</sup> has recently suggested to be so important as to seriously impair the usefulness of SXS as a source of density-of-states information. While such effects are undoubtedly present, we find no grounds for agreeing with this point of view and will now consider the matter in some detail.

The question of the extent to which the inner vacancy destroys the emission spectrum of a metal as a representation of the density of states has been treated from the standpoint of point defect theory.<sup>27,28</sup> Apart from the smearing by the inner level width, the effect of the inner level hole is found to be quite small in comparison with the effect of transition probabilities and inner level width itself. Recently, this viewpoint has been questioned for the lightest metal, lithium<sup>29</sup>; however, Stott and March<sup>30</sup> have reported results suggesting that the anomalously low peak energy in the Li  $K$  spectrum is accountable on the basis of transition probabilities alone.

The effect of the electron-electron interaction on the spectra of "good" metals has been treated by Glick and Longe,<sup>31</sup> and Bose, Glick, and Longe.<sup>32</sup> The major effects are the well-known low-energy tailing of the soft-x-ray emission spectrum, which they are able to account for quantitatively in Na, and the presence of plasmon satellites. If present, the latter are expected to appear at lower energies than the main band, and to be quite weak (on the order of 1% of the main band intensity) due to reduced transition probabilities. Hedin, Lundqvist, and Lundqvist<sup>33</sup> have independently predicted a density-of-states peak due to the occurrence of a resonant hole-plasmon state, lying lower in energy than that predicted by Glick *et al.* Rooke<sup>34</sup> has observed structure displaced by the plasma energy below the main bands of Al, Na, and Mg, but his measurements did not extend down to energies of interest when considering the predictions of Hedin *et al.* Such a peak will presumably be difficult to see because of weak transition probabilities. Our Ni measurements show no clear sign of any low-energy satellites. If present, they are within the noise. There is the distinct tailing of the Ni spectrum which (see Fig. 5) pretty well lies over the  $s$ -band density of states. Actually, the optical data for Ni<sup>35</sup> do not indicate the existence of a well-defined

<sup>25</sup> L. G. Parratt, *Rev. Mod. Phys.* **31**, 616 (1959).

<sup>26</sup> W. E. Spicer, *Phys. Rev.* **154**, 385 (1967).

<sup>27</sup> J. Friedel, *Phil. Mag.* **43**, 152 (1952).

<sup>28</sup> E. Daniel, Doctoral thesis, University of Paris, 1959 (unpublished).

<sup>29</sup> D. A. Goodings, *Proc. Phys. Soc. (London)* **86**, 75 (1965); D. A. Goodings, and B. Mozer, *Phys. Rev.* **136**, A1093 (1964).

<sup>30</sup> M. J. Stott and N. H. March, *Phys. Letters* **23**, 408 (1966).

<sup>31</sup> A. J. Glick and P. Longe, *Phys. Rev. Letters* **15**, 589 (1965).

<sup>32</sup> S. M. Bose, A. J. Glick, and P. Longe, *Bull. Am. Phys. Soc.* **12**, 531 (1967).

<sup>33</sup> L. Hedin, B. I. Lundqvist, and S. Lundqvist, *Solid State Commun.* **5**, 237 (1967).

<sup>34</sup> G. A. Rooke, *Phys. Letters* **3**, 234 (1963).

<sup>35</sup> H. Ehrenreich, H. R. Philipp, and D. J. Olechna, *Phys. Rev.* **131**, 2469 (1963).

<sup>23</sup> H. E. White, *Introduction to Atomic Spectra* (McGraw-Hill Book Company, Inc., New York, 1934), Chap. 16.

<sup>24</sup> J. A. Bearden and C. H. Shaw, *Phys. Rev.* **48**, 18 (1935).

plasmon state, suggesting that the above-mentioned plasmon effects are not to be expected here.

While many-body effects on the SXS of simple metals are reasonably well understood and rather weak, there is some doubt that the transition metals will be so well behaved. The inner vacancy is highly localized and sufficiently long lived so that excitation states with strong effects on the emission spectrum might be expected to occur. This has been suggested as a possible cause of the different widths of the  $L$  and  $M$  emission spectra of the transition metals.<sup>25</sup> We presently show differences in the variation of the transition probabilities as one passes through the  $d$  band to be large enough to account for this. For lack of reasons to the contrary, we currently believe that given the level width smearing, the one-electron model gives a reasonable interpretation of the main peak of the SXS.

Variations in transition probabilities through the  $d$  band and differences in this variation for various experiments are quite important, and as yet, only qualitatively understood. Stott and March's work on Li<sup>30</sup> and Nikifnov's work on the Fe  $L_3$  spectrum<sup>36</sup> appear to be the only available estimates of transition probabilities based on band calculations. The importance of this is illustrated by a rough calculation of the variation of the transition probability through the  $d$ -band of iron. Wood<sup>37</sup> has pointed out that in his augmented plane-wave (APW) calculations for Fe, the  $d$  part of the radial wave function changes from diffuse (or binding) type at the bottom of the band to contracted (or local) at the top, in a fairly smooth manner (see Fig. 3). He notes that this behavior is found in Cu APW functions. From physical bonding arguments, the qualitative features of Fig. 3 are expected to be a general property of the first transition series metals quite independent of any specific calculation. This behavior is expected to decrease in strength for the second and third transition series, where the atomic  $4d$  and  $5d$  states contributing to the top of the  $4d$  and  $5d$  bands are less strongly localized (relative to Wigner-Seitz radii). We have taken Wood's radial wave functions for the top and the bottom of the  $d$  band and normalized them within a sphere of radius  $\rho = 2.5$  a.u., a value lying between the APW and Wigner-Seitz radii. Shown with them in Fig. 3 are  $2p$  and  $3p$  orbitals of Fe,<sup>38</sup> appropriate to the  $L_3$  and  $M_3$  spectra, respectively, and a typical "4p" orbital, appropriate to the photoemission spectrum. From them,

<sup>36</sup> A calculation of the  $L_3$  emission spectrum of Fe has been carried by I. Y. Nikifnov [Fiz. Metal. i Metalloved. 11, 927 (1961)].

Through using different quite rough calculations of the Fe  $d$ -band wave functions, he finds a result in good agreement with that presented here. ( $R_L = 2.2$  as against our estimate of 1.8). He makes no comparison with the  $M_3$  or photoemission spectra.

<sup>37</sup> J. H. Wood, Phys. Rev. 117, 714 (1960).

<sup>38</sup> The atomic orbitals used for the inner state are the  $2p$  and  $3p$  Fe orbitals tabulated in F. Herman and S. Skillman, *Atomic Structure Calculations* (Prentice-Hall, Inc., Englewood Cliffs, New Jersey, 1963). These orbitals are normalized from zero to infinity, but they are quite compact, and so their normalization volume will not affect our results.

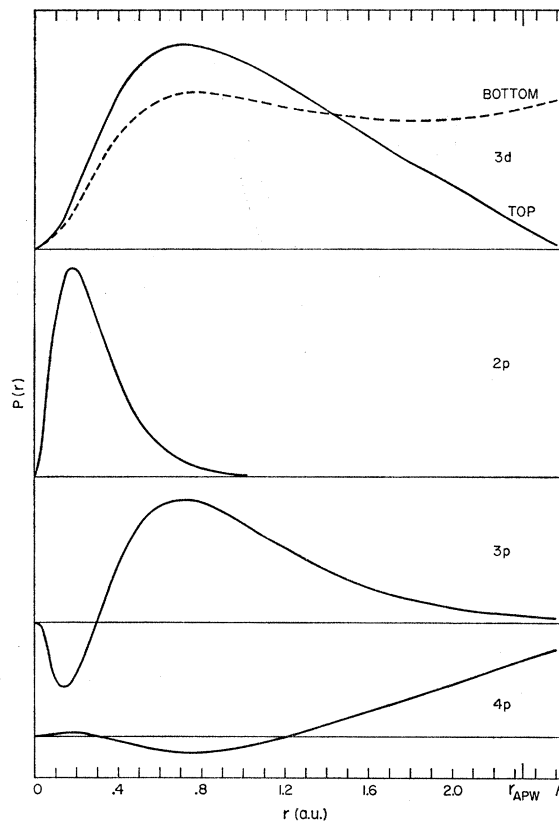


FIG. 3.  $P(r)$ ,  $r$  times the radial wave function, for the bottom and top of the Fe  $d$  band, after Wood, (Ref. 37)  $2p$  and  $3p$  Fe core orbitals, after Herman and Skillman, (Ref. 38) and a typical  $4p$  orbital, a plane wave with  $k=0.5$  a.u., orthogonalized to the Fe core.

we have calculated the radial integral entering the dipole matrix element and in turn the transition probability. For the Fe  $M_3$  spectrum, we find

$$R_M \equiv \frac{|\langle 3p | r | 3d, \text{top} \rangle|^2}{|\langle 3p | r | 3d, \text{bottom} \rangle|^2} = 1.1,$$

where

$$\langle a | r | b \rangle = \int_0^\rho P_a(r) r P_b(r) dr,$$

and

$$\int_0^\rho P_b^2(r) dr = 1.$$

Here,  $P(r) = rR(r)$ , where  $R$  is the radial component of the electron orbital,  $b$  denoting  $d$ -band orbitals, and  $a$  atomic-inner-level orbitals. This result suggests that a truer picture of the density of states can be gotten by a gradual scaling of the  $M_3$  curve, multiplying the low-energy end by a factor of 1.1, with the higher-energy end held at 1.0. This is a small effect for the  $M_3$  spectrum, but is of considerable significance in the  $L_3$  spectrum and the photoemission process. Doing the same calculation for the  $L$  spectrum, with a  $2p$  inner or-

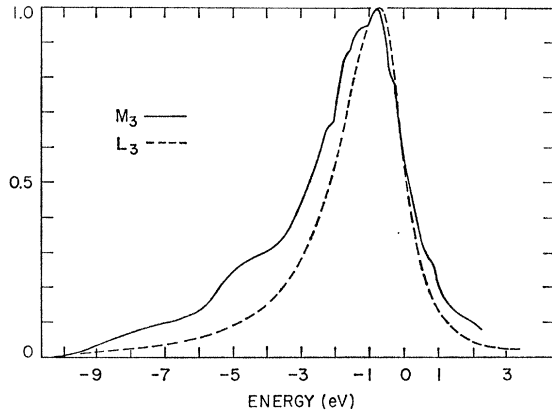


FIG. 4. Comparison of the resolved  $M_3$  band width with the  $L_3$  spectrum of Chopra and Liefeld (Ref. 21).

bital, yields

$$R_L \equiv \frac{|\langle 2p | r | 3d, \text{top} \rangle|^2}{|\langle 2p | r | 3d, \text{bottom} \rangle|^2} = 1.8,$$

quite strong enough to account for the apparent different widths of the transition metal  $M$  and  $L$  emission bands. Simple inspection of Fig. 3 indicates that both  $R_L$  and  $R_M$  should be greater than unity. Cancellation due to the nodal character of the  $3p$  orbital and its tail (in the region,  $r > 1.4$  a.u., where the two  $3d$ 's have crossed over) cause  $R_M$  to be smaller than  $R_L$ . Results applicable to the photoemission spectrum will be discussed in Sec. VI. This, of course, is only a one-center estimate of one aspect of how transition probabilities are affected by orbital character. The  $M$  spectrum samples only the  $s$  (omitted here) and  $d$  components of the band, and actually a significant  $p$  component of varying weight may be present. Many body effects on the matrix elements have also been omitted.

We close this section with a brief discussion of the resolution attained in this work. The combined width of the inner level and valence-conduction band hole states acts to soften and blend any sharp structure in the density of states or transition probabilities. In principle, one can determine this width near the Fermi energy from the width of the corresponding absorption edge, but this is greatly complicated by the energy dependence of the density of states and by structure below the edge due at least in part to absorption or re-emission by valence band electrons. A rough fit to the lower half of the Tomboulian Ni absorption edge<sup>17</sup> can be made with a Lorentzian 0.4-eV wide at half-maximum. However, the resolution in that experiment was limited by the density of lines in the spark radiation source. Inspection of Fig. 1 shows that features about 0.5-eV wide are just resolved. Near the emission peak, our 0.5-Å instrumental window corresponds to a resolution in energy of 0.17 eV. If we attribute the poorer over-all resolution to the combined effects of valence band hole and inner state lifetimes, we again find a width of about 0.4 eV. However, the combined width near  $E_F$  may be

somewhat narrower than this. Unfolding the Ni  $K\beta_{1,3}$  doublet and correcting for instrumental and  $K$  level broadening (estimated from results cited by Parratt<sup>25</sup>) gives an estimate of 0.2 eV for the  $M_3$  hole width. We can safely estimate the combined width near the Fermi level to lie in the range 0.2 to 0.4 eV. Lower in the band it will be much wider. We will make use of these observations in Sec. V.

#### IV. EARLIER WORK AND THE $L$ -SPECTRUM

Earlier work on the Ni  $M_{2,3}$  emission spectrum has generally been done under poor-vacuum conditions and with photographic detection.<sup>39-42</sup> The general features of the early studies, such as location of the peak, width of the band, and to a very limited extent, indications of the structure we observe, agree with the present measurements. Gyorgy and Harvey<sup>40</sup> worked with photoelectric detection and low exciting voltages but made measurements in very poor vacuum during continuous vapor deposition of the sample. Tomboulian's work is of particular interest.<sup>41</sup> His vacuum of  $10^{-6}$  Torr and successive vapor depositions of the sample on a cooled substrate permitted short runs between depositions during which the Ni surface should remain relatively clean. However, he used photographic detection with its poorer (about 2% at best) linearity of response, and although the sample was cooled, did not monitor the sample surface temperature. Although the magnetic state of his sample is in doubt, it is perhaps worth mentioning that our data can be fitted to his in the region about the peak by assuming an exchange splitting of about 0.3 eV. Clearly, it is most desirable to record the  $M_{2,3}$  emission spectrum of clean Ni in the ferromagnetic state, a task we are not yet equipped to perform.

Comparison with the corresponding  $L$  emission spectrum is particularly important for the two measurements are complementary. In the  $L$  spectra,  $L_3$  and  $L_2$  sub-bands and multiple ionization satellites do not overlap but the combined lifetime and instrumental smearing is large, and fine detail cannot be seen; in the  $M$  spectra, better resolution can be had, but bands and satellites overlap. In Fig. 4, we compare our resolved  $M_3$  band with the  $L_3$  band of Ni measured by Chopra and Liefeld<sup>21</sup> at 800°C and threshold excitation. Electron beam incidence and photon take-off angles were both 90°. The spectrum is free of satellite and self-absorption effects. There may be some oxide contamination effects present. By their technique of studying the  $L_3$  band as a function of voltage down to the excitation threshold voltage, these authors have shown the occurrence of

<sup>39</sup> H. W. B. Skinner, T. G. Bullen, and J. E. Johnston, *Phil. Mag.* **45**, 1070 (1954).

<sup>40</sup> E. M. Gyorgy and G. G. Harvey, *Phys. Rev.* **93**, 365 (1954).

<sup>41</sup> D. E. Bedo and D. H. Tomboulian, *Phys. Rev.* **121**, 146 (1960).

<sup>42</sup> J. Clift, C. Curry, and B. J. Thompson, *Phil. Mag.* **8**, 593 (1963).

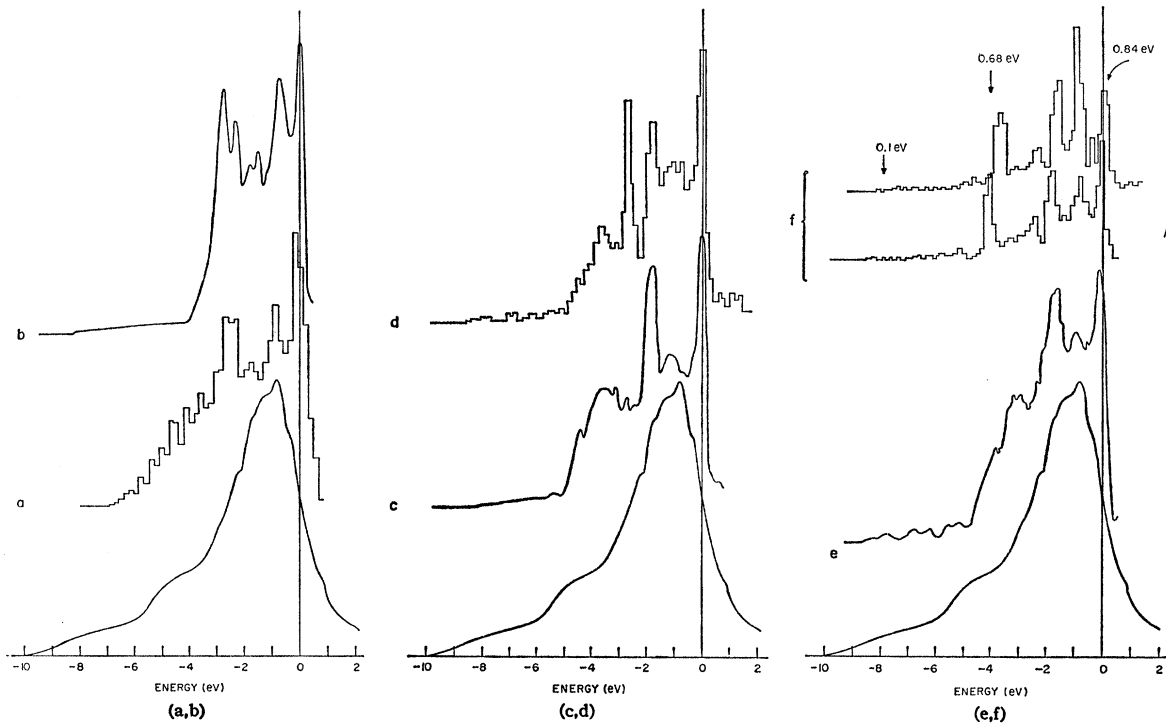


FIG. 5. Comparison of the  $M_3$  band with various calculated densities of states (for identification and discussion, see Ref. 43): (a,b)  $M_3$  band compared with interpolated, unhybridized density-of-states calculations; (c,d)  $M_3$  band compared with interpolated, hybridized density-of-states calculations; and (e,f)  $M_3$  band compared with first-principles APW density-of-states calculations, based on a limited sampling of the zone.

multiple valence band vacancy satellite smearing of the emission edge quite clearly, and their measurements indicate that this effect distorts the band noticeably only above the Fermi energy. The lack of structure in the  $L_3$  band can be ascribed to poorer resolution. A Lorentzian with width at half maximum of 1.0 eV gives a good fit to the  $L_3$  high-energy edge, as experimentally presented, including instrumental broadening.

As we have pointed out in Sec. III, the narrower overall width of the  $L_3$  band is, in all likelihood, due simply to differences in the systematic variation through the band of the  $3d \rightarrow 2p$  and  $3d \rightarrow 3p$  transition probabilities. We argued there that a better picture of the single-particle density of states could be gotten from the  $M_3$  band by multiplying the low-energy end of the  $d$ -part by 1.1, while holding the high-energy end fixed at 1. A larger factor of 1.8 applies to the  $L$  spectrum, and this is in the right direction and of sufficient size to account for its apparent narrower width.

## V. RESULTS COMPARED WITH PREDICTED DENSITIES OF STATES

In Figs. 5 the resolved  $M_3$  band is compared directly with the various calculations of the density of states of paramagnetic Ni. The curves (a) and (b) of Fig. 5 are the results of interpolating early first-principles band calculations using a fine Brillouin zone mesh, but not allowing for band hybridization. The curves (c) and (d)

of Fig. 5 are again interpolated using the same fine mesh, but including hybridization. In (e) and (f) of Fig. 5, we show the results of two recent first principles calculations employing a much smaller sampling of the zone.<sup>48</sup>

<sup>48</sup> Curve (a) is from E. D. Thompson and J. J. Meyers [Phys. Rev. 153, 574 (1966)], who used the Slater-Koster interpolation scheme to fit Hanus's first-principles band calculations (See Ref. 3). Hybridization parameters were set equal to zero. Curves (b) and (c) are from Hodges *et al.* (See Ref. 4) using a new interpolation scheme, again fitting the Hanus Ni bands. Curve (b) is unhybridized, while (c) is hybridized. Curve (d) is that of Wakoh and Yamashita (See Ref. 5) using a new interpolation scheme to their own first-principles Green's-function calculation for Ni. The bands are hybridized. All of these interpolated calculations used a mesh of 16 384 points in the Brillouin zone. Curve (e) is a first-principles calculation, done at 2084 zone points, an extension of the work of Snow *et al.* (See Ref. 6) in their investigation of the sensitivity of the Ni Fermi surface to the assumed electronic configuration. The Fermi surface associated with curve (e) gives a realistic fit to the area of the necks at the (111) zone faces. The curves (f) are from the calculations of Connolly (See Ref. 7) on ferromagnetic Ni using 256 points in the zone. He used different potentials for up and down spins, and the splitting of the bands is not rigid. To indicate the paramagnetic result we have shifted the majority spin curve by the 0.8-eV splitting near the Fermi energy, and indicated the splitting in the middle and at the bottom of the band. Connolly varied the numerical coefficient of the  $\rho^{1/3}$  exchange potential to fit the observed magneton number and electronic specific heat of Ni. We compare his maximum splitting to the rigid splitting of 0.7 eV used by Wakoh and Yamashita to fit the area of the (111) neck, and the maximum value of 0.37 eV found (in the nonrigid approximation) by Hodges *et al.*, who used a variety of experimental results to fit the coefficients in their interpolation scheme. We finally note that INS (See Ref. 9) and PES (See Ref. 8) measurements above the Curie temperature indicate that the splitting can be no more than a few tenths of an eV.

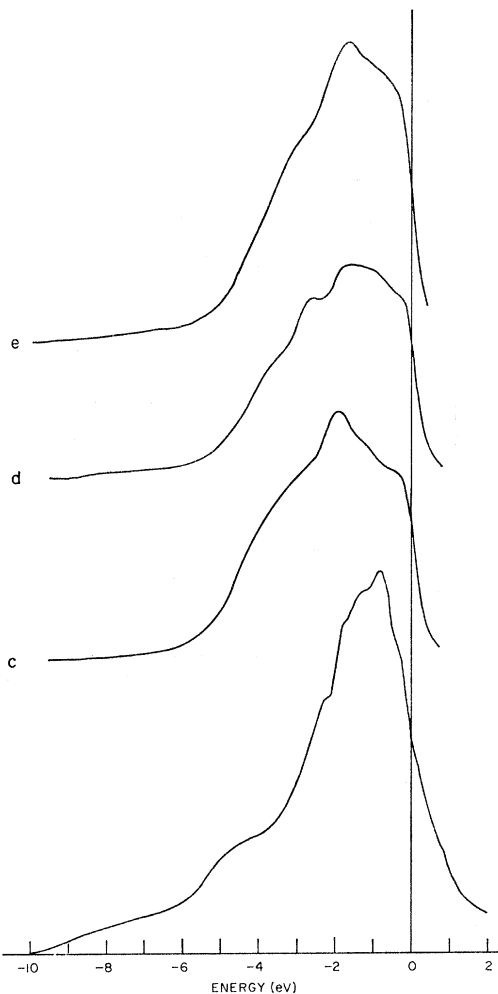


FIG. 6. Density-of-states curves *c*, *d*, and *e* of Fig. 5 are multiplied by the Fermi distribution function at 960°C and folded into a Lorentzian smearing function whose width is energy-dependent: 0.4 eV at  $E_F$ , to 1.0-eV wide at the bottom of the band. Comparison is made with the  $M_3$  band. No allowance for transition-probability variation is made here.

Omitting detail, qualitative agreement is found between the interpolated and first-principles calculations. All have a sharp peak at the Fermi energy and the total band widths are in fair accord. Detailed structure is strongly dependent on  $s$ - $d$  hybridization. (Note the marked differences between curves *b* and *c* of Fig. 5, which differ only in this respect.) Lack of detailed structural agreement among the various curves should not be taken as either surprising or discouraging.

The over-all SXS  $d$ -band width is in reasonable accord with the calculated curves, as are those of INS and PES as well, as reference to Fig. 7 will show. Indications of detailed structural agreement with any of the calculated curves is scant. Rather than a peak just below  $E_F$ , we observe a distinct shoulder. Below  $E_F$ , the  $M_3$  band shows considerable partially resolved detail, particularly the small peak at  $-1$  eV and the distinct shoulder at about  $-2.3$  eV.

No distinct peaks are seen in the region of  $-4$  to  $-2$  eV. While the calculated curves disagree on the structure in this region, they all indicate some. To some extent, this can be accounted for by the finite resolution of the experiment. First, the 10–90% width of the Fermi distribution function at 960°C is 0.47 eV, and the predicted peak at the Fermi edge is narrow. Observation of a noticeable shoulder at the edge can be considered agreement with theory. Secondly, the resolution of a soft-x-ray emission experiment is by no means constant throughout the emission band. The final valence-conduction band hole state of the emission process will be long-lived near the Fermi level, but due to Auger filling, hole lifetime becomes progressively shorter as one goes deeper in the band. This effect, which gives rise to the well known tailing of soft-x-ray emission bands, should be properly computed by the methods of Glick *et al.*<sup>31,32</sup> A rough study can be made by applying an energy-dependent Lorentzian smearing function to the calculated density of states curves.<sup>44</sup> As has been discussed in Sec. III, the Ni absorption data<sup>17</sup> and the apparent resolution of the emission spectrum near  $E_F$  suggests that the combined inner level and conduction band hole width lies in the range of 0.2 to 0.4 eV near  $E_F$ . In the simple metals, hole states at the bottom of the band have a width of about 1.0 eV. (The appropriate value for Ni may be larger, in view of the greater number of electrons in the  $s$ - $d$  bands.) The simplest approximation one can make is to let the Lorentzian smearing width vary from 0.4 to 1.0 eV as a linear function of the number of filled states in the  $s$ - $d$  band above the hole level in question, thereby accounting for inner level and conduction band lifetimes.<sup>44</sup> Figure 6 shows the result of applying such an energy-dependent smearing function to curves *c*, *d*, and *e* of Fig. 5. Allowance has been made for the Fermi distribution function in each case. The sharp peaks at about  $-2.5$  eV are softened considerably in each case, although not washed completely into shoulders, while the peak at  $E_F$  survives only as a shoulder in the band. The Fermi function significantly contributes to this. A similar calculation using a width of 0.25 eV at the Fermi level strengthens this shoulder very slightly. No allowance has been made here for variation in transition probability, and the presence of any varying  $p$ -component in the bands is ignored. Collective effects are considered only in the rough approximation of the energy-dependent window function. While other factors may enter, it currently appears unnecessary to invoke them when considering the rounding of the SXS spectrum at  $E_F$ .

<sup>44</sup> Two temperature effects, one of which is an extra broadening mechanism, have been suggested by Ehrenreich (private communication). Using tight-binding arguments of Heine one would expect the increase in lattice constant (on going from 0 to 1273°K) to produce a narrowing of the  $d$  bands by about 0.4 eV, a small effect. Secondly, lattice vibrations represent substantial deviations in lattice spacing, and use of the same criterion suggests another broadening which might approach 0.4 eV, presumably of Gaussian form. Parratt (See Ref. 25) has also discussed lattice broadening.

There is the possibility of improving the resolution of the SXS measurements. Since the major limitation on resolution is the broad smearing function, any attempt at improving spectrometer resolution seems pointless. Unfolding procedures to remove the effect of an (assumed) smearing function would be less fruitful than asking theory to provide a better quantitative *a priori* estimate of the spectrum in all its aspects.

## VI. RESULTS COMPARED WITH INS AND PES

Let us compare the Ni SXS  $M_3$  band, the INS unfold function of Hagstrum and Becker,<sup>9</sup> and the "optical" density of states deduced by Blodgett and Spicer from their PES results.<sup>8</sup> Such a comparison is by no means trivial since different initial states and transition probabilities (and many body effects) are at play. As with the preceding section, emphasis will be placed on making this comparison in the single-particle approximation. INS is more sensitive to the mobile  $s$ - $p$  electrons than to the more highly localized  $d$ -electrons, and details of band structure are expected to be lost in the complex unfolding procedure. The PES density-of-states curve is gotten in a much simpler manner, involving the assumption of nondirect transitions (non- $k$ -conserving transitions, in the single-particle sense) and a single constant transition probability, independent of initial and final states. A rough but meaningful comparison can be made by normalizing each curve at its peak value, as is done in Fig. 7. On this basis, INS and SXS are seen to be in fair accord as to the location and width of the  $d$  band, and neither show the very large peak seen at  $-4.5$  eV in the PES curve. INS and SXS, as well as the band calculations, indicate that there are  $d$  states at this energy, but none suggests the existence of such a dominant strong peak. The assumptions yielding the PES curve were employed for the good reason that they are consistent with the behavior of the raw PES data with varying incident photon energy. The assumptions of nondirect transitions and transition probabilities independent of final (but not initial) state are essential to the analysis yielding the PES curve of Fig. 7. Detailed inspection of these assumptions is beyond the scope and intent of this paper, but it is our view that a spectrum of this origin is surprising if only because of the asserted unimportance of  $k$ -conserving transitions for  $d$  bands. We feel that no adequate physical rationalization of this has yet appeared in the literature. Some observations of other workers will, of necessity, be noted but we will not develop our views on this matter here.

Comparison of the three curves of Fig. 7 (accepting the procedures yielding them) with the intent of learning something of the single-particle density of states requires that two factors be considered: first, any warping by single particle transition probabilities, and second, multiparticle effects. A good deal has already been said on the bearing of these matters to the SXS

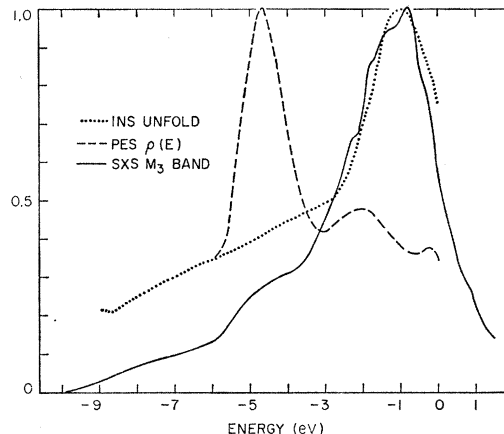


Fig. 7. Comparison of the  $M_3$  band with the INS unfold function (Ref. 9) and the density of states deduced from PES (Ref. 8). Each curve is normalized at peak value.

results. Similar inspection of the PES curve seems desirable in view of the gross discrepancy between it and the other experimental curves.

Variation of transition probability with initial state is definitely allowed in the PES analysis, and will warp the curve in Fig. 7. The implications of such warping have not been indicated in any of the PES work but we believe them to be exceedingly important. The radial variation in the  $d$  bands which leads to sharp differences in the widths of  $L$  and  $M$  emission spectra should produce pronounced warping in the PES as well. Again making the oversimplified assumption of a dipole operator (and the one-center approximation), we calculate the effect of this radial variation in Fe, which shows a similar somewhat weaker low-energy PES peak,<sup>45</sup> to be

$$R_{\text{PES}} \equiv \frac{|\langle 4p|r|d, \text{top} \rangle|^2}{|\langle 4p|r|d, \text{bottom} \rangle|^2} = 0.07 \text{ to } 0.10,$$

where the ratio has been evaluated for a variety of  $4p$ -like orbitals.<sup>46</sup> Granting the assumption of indirect transitions this cannot be the full story, but if we take this ratio seriously, it suggests a much stronger, and opposite, warping of the PES results due to this source than for either the  $L_3$  or  $M_3$  x-ray spectra. If the integrals entering the PES has been extended out to the Wigner-Seitz radius,  $R_{\text{PES}}$  should become smaller still. The nature and strength of this behavior could have been predicted simply by inspection of Fig. 3. The  $4p$  orbital samples the  $d$  orbitals most strongly in the interstitial region, beyond the crossover point where their variation is most pronounced. The nodal character

<sup>45</sup> W. E. Spicer, in *Optical Properties and Electronic Structure of Metals and Alloys*, edited by F. Abeles (North-Holland Publishing Company, Amsterdam, 1966), p. 308.

<sup>46</sup> These were the  $p$  components of various plane waves orthogonalized to the ion core. The  $k$  values were those appropriate to free-electron spheres enclosing from two to three free electrons per atom. A calculation with an atomic  $4s$  function yielded results of similar character.

of the  $4p$  function further enhances the effect, since the entire region outside  $r=0.3$  a.u. contributes cooperatively to  $R_{\text{PES}}$ . Quite aside from any shortcomings in the calculations, Fig. 3 and bonding considerations suggest that the direction and *relative* strength of the  $R_{\text{PES}}$  effect is correct.

Assuming that the PES peak at  $-4.5$  eV is associated with a simple, single-particle density of states, the ratio  $R_{\text{PES}}$  implies that it has been spuriously enhanced by an order of magnitude relative to the top of the band by transition probabilities. Even with the strong reduction indicated here, some peaking is expected to remain.

In Sec. III, we enumerated reasons for believing that the main SXS structure can be attributed to single-particle processes, multiparticle effects being separated off in the low-energy region. In contrast with the usual procedure in the literature of considering the PES curve as typical of the single-particle density of states, Spicer *et al.*<sup>47</sup> have instead correlated the strong peak with multiparticle effects.

Stanford, Arakawa, and Birkhoff<sup>48</sup> have measured the PES of unexcited Ag up to 22.3-eV photon energy, and have found a small peak about 7.5 eV below the main band. They interpreted this as a satellite of the main  $d$ -band peak, associated with the characteristic energy loss observed in Ag at 7.5 eV which may be attributed to a strong, direct interband transition. There is a suggestion of structure in the Ag optical data at this energy. Optical constants measurements on Ni show a strong peak in  $2\omega nk$  at 4.5 eV,<sup>35</sup> and energy-loss measurements show a characteristic loss at about the same energy.<sup>49</sup> Analogy to the Ag case suggests that part of the observed low-energy PES peak is due to the same type of energy loss. Spicer has presented reasons for thinking this unimportant.<sup>50</sup> Whatever the source, there is a definite correlation between low-energy PES peaks and structure in the optical properties of such metals.<sup>45,48</sup> This is hardly surprising in view of the common excitation mechanism.<sup>51</sup>

Mott<sup>51</sup> has suggested an alternative mechanism for the low-energy PES peak. He proposes that a significant mixture of  $3d^8 4s^2$  character may occur in the many electron wave function of metallic Ni, and pictures the large PES peak as arising from photoexcitation of a  $d$  electron from a Ni atom in the  $3d^8$  configuration. The final state consists of two  $d$ -band holes and two electrons in excited states. He gives physical arguments

<sup>47</sup> W. E. Spicer, W. F. Krolkowski, and A. Y-C. Yu, *Bull. Am. Phys. Soc.* **12**, 287 (1967).

<sup>48</sup> E. T. Arakawa, colloquium, National Bureau of Standards, 1967 (unpublished). Much the same material appears in J. L. Stanford, E. T. Arakawa, and R. D. Birkhoff, Oak Ridge National Laboratory Report no. ORNL-TM-1392, 1966 (unpublished).

<sup>49</sup> J. L. Robins and J. B. Swan, *Proc. Phys. Soc. (London)* **76**, 857 (1960).

<sup>50</sup> C. N. Berglund and W. E. Spicer, *Phys. Rev.* **136**, A1030 (1964); **136**, A1044 (1964).

<sup>51</sup> N. F. Mott (unpublished). Professor Mott is quoted on this point in *Optical Properties and Electronic Structure of Metals and Alloys*, edited by F. Abeles (North-Holland Publishing Company, Amsterdam, 1966), p. 314.

based on the initial states of the systems to explain why this effect is seen in PES and optical constants measurements, but not in SXS and INS.

The present authors<sup>10,52</sup> have independently suggested a double photoexcitation which may be closely related to one or the other of the above processes. If the optical peak and energy loss at 4.5 eV in Ni are due to a strong direct interband transition, (possibly<sup>35</sup>  $L_1 \leftrightarrow L_2$ ), two electrons may be excited by a single photon, one electron making the strong direct transition, the other carrying the balance of the energy. This double hole excitation, aided by a strong direct transition, can be viewed (and is experimentally indistinguishable) as either an extension of the Mott process, causing or rather assisting its appearance experimentally, or a quite different process; for example, a single excitation followed by energy loss to a direct interband transition of much the type discussed by Arakawa.

Multiparticle effects in the collective sense, as treated by Glick *et al.*,<sup>31,32</sup> and Hedin *et al.*,<sup>33</sup> are not apparent in the SXS or INS measurements, save for the low-energy tailing of the  $M_3$  band. Phillips has argued for a deep band "resonance" resulting from "maximal atomic correlation" at the resonance energy.<sup>53</sup> Hagstrum has pointed out<sup>9</sup> that such a "resonance" should appear in INS as well as PES. Not seeing it in INS, he concluded that the PES peak is not of this origin. Phillips<sup>53</sup> expressed the opinion that this effect appears in the SXS, but as the present authors<sup>10</sup> have pointed out, this interpretation of SXS is erroneous for it employs a distortion of the energy scale by a factor of three, well outside any effect which may be attributed to the inner level vacancy and it misplaces the Fermi energy by some 7 eV (as determined by Tomboulia's absorption data<sup>17</sup>). In contrast with Hagstrum's conclusion, Spicer and coworkers<sup>47</sup> have recently discussed the PES data in terms of Phillip's mechanism. Their choice was based on certain systematics (as a function of metal observed) in the PES results.

In this section we have compared the several experimental curves of Fig. 7 and have seen significant discrepancies between them. We have superficially inspected warping due to varying transition probabilities, and the results suggest that it is more severe for the PES than the SXS results. We have also surveyed multiparticle effects one or another of which are currently thought (e.g., see Refs. 26 and 47) to make significant contributions to the PES curves. It should be noted that the optical peaks in Ni (4.5 eV) and Ag (7.5 eV) have been attributed to *direct* transitions by Ehrenreich and Phillip,<sup>35,54</sup> and the same suggestion has recently been made for Ni by Mueller and Phillips.<sup>55</sup>

<sup>52</sup> This model predicts a PES peak at  $-7.5$  eV in Ag. In Ref. 10, we gave a value of  $-6.1$  eV based on erroneous interpretation of Ag optical data.

<sup>53</sup> J. C. Phillips, *Phys. Rev.* **140a**, A1254 (1965).

<sup>54</sup> H. Ehrenreich and H. R. Philipp, *Phys. Rev.* **128**, 1622 (1962).

<sup>55</sup> F. M. Mueller and J. C. Phillips, *Phys. Rev.* **157**, 600 (1967).

This has obvious implications for PES behavior as well, and Arakawa has in fact suggested<sup>48</sup> that such direct transitions are responsible for a small peak in the Ag PES curve. To the extent that direct transitions from the  $d$  bands are present, the data reduction yielding the PES curve in Fig. 7 is incomplete.

We believe that, of the curves of Fig. 7, the SXS and INS are closer in describing the single-particle density of states of Ni than is the PES curve.

## VII. CONCLUSIONS

In the present work, the  $M_{2,3}$  emission spectrum of clean, paramagnetic Ni has been measured, and the  $M_3$  band resolved in a plausible way from the overlapping continuum,  $M_2$  band, and satellites. The resulting  $M_3$  band shows fine structure. No major experimental breakthrough has been made here, but the state of the art has been pushed to the point where comparison with other techniques is fully warranted.

We believe that SXS and INS are indeed providing useful information on the single-particle density of states. To the extent that the PES results do not reflect severe transition probability warping and/or occurrence of direct transitions (to date omitted from the analysis of the  $d$ -band density of states), the multiparticle effects<sup>47</sup> are of considerable interest. Direct information on the density of states from this source is limited until such effects are resolved out of the experimental curves. In all cases, comparison with theory yields but crude qualitative agreement, and further comparison requires predictions of transition rates (and of level widths for the SXS) as well as densities of states. Until such comparisons are made, detailed discrepancies between

theory and experiment cannot be taken seriously. The level width smearing of the density of states, as seen in Fig. 6, does not necessarily make the SXS investigations less useful than alternate techniques, which themselves require unfolding techniques potentially no less severe. The level width smearing *is* the folding associated with the SXS problem. Comparison between theory and experiment will become straightforward once it is quantitatively understood. Even with the smearing present, there should remain a distinct correlation between shoulders in the SXS curves and strong structure in the "true" density of states. It must be emphasized that much of this smearing is associated with the low-lying conduction band states, and *any and all* experiments exciting holes in these states will suffer such smearing.

The crude agreement for the experiments least affected by multiparticle and other effects supports the validity of the single particle picture for at least some properties, off the Fermi surface, of a metal such as Ni.

## ACKNOWLEDGMENTS

We are particularly indebted to Dr. R. D. Deslattes for advice and council on this work. Thanks are due Dr. L. H. Bennett for discussions and encouragement, and to Professor H. Ehrenreich for a critical reading of the manuscript. We also thank Professor W. E. Spicer, Dr. H. D. Hagstrum, E. C. Snow, Dr. A. J. Glick, Dr. S. Lundqvist, and Dr. E. T. Arakawa for discussions and correspondence, and for furnishing results prior to publication during the course of our work. J. E. McLane gave us considerable assistance with reduction of the data.